npg

Intact memory in TGF-β1 transgenic mice featuring chronic cerebrovascular deficit: recovery with pioglitazone

Nektaria Nicolakakis[1,4], Tahar Aboulkassim[1,4], Antonio Aliaga[2], Xin-Kang Tong[1], Pedro Rosa-Neto[2,3] and Edith Hamel[1]

[1]Laboratory of Cerebrovascular Research, Montreal Neurological Institute, McGill University, Montréal, Quebec, Canada; [2]Brain Imaging Centre, Montreal Neurological Institute, McGill University, Montréal, Quebec, Canada; [3]Douglas Hospital Research Centre, McGill University, Montréal, Quebec, Canada

The roles of chronic brain hypoperfusion and transforming growth factor-beta 1 (TGF-β1) in Alzheimer's disease (AD) are unresolved. We investigated the interplay between TGF-β1, cerebrovascular function, and cognition using transgenic TGF mice featuring astrocytic TGF-β1 overexpression. We further assessed the impact of short, late therapy in elderly animals with the antioxidant N-acetyl-L-cysteine (NAC) or the peroxisome proliferator-activated receptor-γ agonist pioglitazone. The latter was also administered to pups as a prophylactic 1-year treatment. Elderly TGF mice featured cerebrovascular dysfunction that was not remedied with NAC. In contrast, pioglitazone prevented or reversed this deficit, and rescued the impaired neurovascular coupling response to whisker stimulation, although it failed to normalize the vascular structure. In aged TGF mice, neuronal and cognitive indices—the stimulus-evoked neurometabolic response, cortical cholinergic innervation, and spatial memory in the Morris water maze—were intact. Our findings show that impaired brain hemodynamics and cerebrovascular function are not accompanied by memory impairment in this model. Conceivably in AD, they constitute aggravating factors against a background of aging and underlying pathology. Our data further highlight the ability of pioglitazone to protect the cerebrovasculature marked by TGF-β1 increase, aging, fibrosis, and antioxidant resistance, thus of high relevance for AD patients.

Introduction

Chronic cerebral hypoperfusion is a typical feature of Alzheimer's disease (AD) (Bell and Zlokovic, 2009) capable of predicting clinical evolution (Hirao et al, 2005) and response to medication (Yoshida et al, 2007). Whether reductions in cerebral blood flow (CBF) can cause AD, however, remains an open question. Evidence from human studies or vessel occlusion/stenosis paradigms in rodents has pointed to an association between substrate deprivation and memory impairment (Ruitenberg et al, 2005; Farkas et al, 2007; Miki et al, 2009), yet the high degree of hypoperfusion and neuronal loss has often confounded interpretation of these results. In AD, the decrease in CBF may be related to a lower demand by the afflicted brain tissue and/or to compromised vascular networks. Examples of the latter have been cited in patients with AD or in mouse models. They include sequestration of vaso-dilators by free radicals (Iadecola et al, 1999; Tong et al, 2005), disruption of vascular smooth muscle by the amyloid-β peptide (Han et al, 2008), degeneration of vasodilatory perivascular cholinergic afferents (Tong and Hamel, 1999), and cerebrovascular fibrosis caused by extracellular matrix protein accumulation in basement membranes (Christov et al, 2008). Furthermore, elevations of transforming growth factor-beta 1 (TGF-β1), a key extracellular matrix regulator, have been documented in the brain and the cerebral

vasculature of AD patients (Wyss-Coray et al, 1997; Grammas and Ovase, 2002), and in groups at risk of developing AD, i.e., hypertensive, diabetic, or ischemic stroke patients (Krupinski et al, 1996; Peterson, 2005). TGF-β1 receptor levels and signaling are altered in the AD brain and mouse models (Tesseur et al, 2006), and TGF-β1 gene polymorphisms may increase AD risk (Dickson et al, 2005). Interestingly, transgenic mice overexpressing TGF-β1 in the brain (TGF mice) develop AD-like vascular structural changes (Wyss-Coray et al, 1995), impaired vasodilatory and contractile ability (Tong et al, 2005), baseline cerebral hypoperfusion (Gaertner et al, 2005), and hypometabolism (Galea et al, 2006), although to date, neuronal and cognitive functions have not been assessed in these mice.

We sought to investigate the relevance of TGF-β1 increase for cerebrovascular and neuronal/cognitive markers, and the impact of prophylactic or therapeutic intervention with the antioxidant N-acetyl-L-cysteine (NAC) or the peroxisome proliferator-activated receptor-γ agonist pioglitazone. These compounds were selected for their efficacy against cerebrovascular dysfunction in an AD mouse model of amyloidosis (Nicolakakis et al, 2008). Pioglitazone was additionally chosen for its potential to remedy fibrosis in TGF mice through its transcriptional influence over proteins regulating extracellular matrix turnover (Fu et al, 2001). We specifically studied arterial responsiveness and proteins regulating vascular structure or function. We also measured the neuronally driven cerebral glucose uptake (CGU) and CBF responses to whisker stimulation, the status of astrocytes involved in synaptic transmission and neurovascular coupling (Haydon and Carmignoto, 2006), cortical cholinergic innervation, not only known for its effect on cognition and CBF but also for its susceptibility to ischemia (Craft et al, 2005), and spatial memory in the Morris water maze. Our results provide new insights into the link between cerebrovascular dysfunction and dementia, and support the use of pioglitazone as a strategy to preserve the cerebral circulation in the context of advanced age, fibrosis, and antioxidant resistance, hence to potentially delay disease progression in vulnerable populations or to improve response to AD therapies.

Materials and methods

Reagents and Antibodies

Pioglitazone was generously provided by Takeda Pharmaceuticals North America, Inc (Chicago, IL, USA), and was mixed in Teklad Rodent chow diet no. 2019 by Research Diets (New Brunswick, NJ, USA). N-acetyl-L-cysteine (NAC) was obtained from Sigma-Aldrich (St Louis, MO, USA). The remaining reagents were serotonin (5-HT), acetylcholine (ACh), sodium nitroprusside (SNP), and L-NNA (N^{ω}-nitro-L-arginine) from Sigma-Aldrich; calcitonin

gene-related peptide (CGRP) and endothelin-1 (ET-1) from American Peptide (Vista, CA, USA); and ketamine from Wyeth (St-Laurent, QC, Canada). Antibodies were rabbit anti-endothelin-B receptor (ET$_B$; Alomone Labs, Jerusalem, Israel), anti-connective tissue growth factor (CTGF; Abcam, Cambridge, MA, USA), anti-M5 mAChR (anti-M5 muscarinic ACh receptor; Research and Diagnostics, Las Vegas, NV, USA), anti-glucose transporter-1 (Millipore, Temecula, CA, USA), anti-glial fibrillary acidic protein (GFAP; Dako, Mississauga, ON, Canada), anti-cyclooxygenase 2 (Cayman, Ann Arbor, MI, USA), anti-collagen IV (for western blots; Rockland Immunochemicals, Gilbertville, PA, USA) or goat anti-collagen IV for immunohistochemistry (Millipore), anti-choline acetyltransferase (ChAT; Millipore), mouse anti-endothelial nitric oxide synthase (NOS) (BD Biosciences Transduction Laboratories, Mississauga, ON, Canada), and anti-β-actin (Sigma-Aldrich). Biotinylated secondary antibodies, the avidin–biotin complex (ABC kit, Vectastain Elite), 3,3′-diaminobenzedene (DAB), and slate gray kits were purchased from Vector Labs (Burlingame, CA, USA). Horseradish peroxidase-conjugated and donkey anti-rabbit cyanin 2-conjugated secondary antibodies were obtained from Jackson ImmunoResearch (West Grove, PA, USA). The Enhanced ChemiLuminescence (ECL) Plus kit was from GE Healthcare (Piscataway, NJ, USA), and Correlate-EIA Corticosterone enzyme immunoassay kit was from Assay Designs (Ann Arbor, MI, USA).

Animals and In Vivo Treatments

Experiments were approved by the Animal Ethics Committee of the Montreal Neurological Institute, and respected guidelines of the Canadian Council on Animal Care. We used heterozygous transgenic mice overexpressing a constitutively active form of TGF-β1 under the control of the GFAP promoter on a C57BL/6J background (line T64) (Wyss-Coray et al, 1995; Tong et al, 2005). Transgene expression was confirmed with touchdown PCR using tail-extracted DNA (Wyss-Coray et al, 1997; Tong et al, 2005). Elderly mice ($\sim$18 months) were treated with blood–brain barrier-permeable NAC (100 mg/kg per day, intraperitoneally in phosphate-buffered saline for 4 weeks) or pioglitazone (20 mg/kg per day, per os, 6 to 8 weeks), with half of the wild-type and TGF mice in each group receiving vehicle or control diet. In one cohort, mice were kept on pioglitazone for up to 16 weeks to allow for positron emission tomography (PET) scanning (see below). These treatments will be referred to as 'short' for the remainder of this paper. Structural alterations may be difficult to reverse at an advanced age, but could be amenable to prophylactic treatment; hence, $\sim$4-week-old pups were placed on pioglitazone for 1 year (referred to as 'long' treatment), and tested when $\sim$12 months old. Mice had access to water and food ad libitum, and showed no significant change in body weight (g) or fasting glycemia (mmol/L) at the end of treatment (Supplementary Table 1), the latter was measured in the pioglitazone cohorts with a commercial glucometer (One Touch Ultra, LifeScan, Burnaby, BC, Canada) using blood collected from the tail tip. The only exception was the slightly higher weight gain

in wild-type animals ($\sim 75\%$) compared with all other groups ($\sim 65\%$) after 1 year of pioglitazone treatment (Supplementary Table 1).

Vascular and Brain Tissues

After treatment and/or *in vivo* testing, mice were killed by cervical dislocation and the reactivity of the middle cerebral artery tested (see below), while pial vessels (circle of Willis and its ramifications) were removed and stored ($-80°C$) for subsequent protein extraction. The brains were immersion-fixed overnight (at $4°C$ in 4% paraformaldehyde in 0.1 mol/L phosphate-buffered saline, pH = 7.4), cryoprotected, frozen in isopentane, and stored ($-80°C$) until cutting of 25-μm-thick free-floating coronal sections on a freezing microtome for immunohistochemistry. Some pioglitazone-treated mice and untreated controls were perfused intracardially (4% paraformaldehyde) under deep anesthesia (65 mg/kg sodium pentobarbital, intraperitoneally), and their brains were processed for paraffin embedding and microtome cutting of 5-μm-thick coronal sections.

Vascular Reactivity

The reactivity of isolated, cannulated, and pressurized middle cerebral artery segments was evaluated using online videomicroscopy, as described previously (Tong *et al*, 2005; Nicolakakis *et al*, 2008). Dilatory responses to ACh (10^{-10} to 10^{-5} mol/L) and CGRP (10^{-10} to 10^{-6} mol/L) were tested on vessels preconstricted submaximally with 5-HT (2×10^{-7} mol/L). Contractile responses to ET-1 (10^{-10} to 10^{-6} mol/L) and tonic production of the vasodilator NO were evaluated in vessels at basal tone, the latter by measuring diameter decrease during L-NNA-mediated inhibition (10^{-5} mol/L, 35 minutes) of NOS. The integrity of the smooth muscle was evaluated by testing arterial relaxation to the NO donor SNP (10^{-10} to 10^{-4} mol/L). Percentage change in vessel diameter from either the basal or preconstricted tone was plotted as a function of agonist concentration or time course of NOS inhibition. The maximal vessel response (EA_{max}) and the concentration eliciting half of the EA_{max} (EC_{50} value or $pD_2 = -(\log EC_{50})$) were used to determine agonist efficacy and potency, respectively.

Western Blot

Protein changes were investigated in pial vessels by western blot as in our earlier study (Nicolakakis *et al*, 2008). Membranes were loaded with proteins (4 to 5 μg), and incubated overnight with rabbit anti-ET_B receptor (1:400), anti-collagen IV (1:1,000), anti-CTGF (1:200), anti-M5 mAChR (1:400), anti-glucose transporter-1 (1:400) or mouse anti-endothelial NOS (1:500), anti-cyclooxygenase 2 (1:200), or anti-β-actin (1:10,000) that was used to normalize loading variation. Blots were incubated with horseradish peroxidase-conjugated secondary antibodies (1:2,000 or 1:4,000, 1 hour), and proteins were visualized with ECL using phosphorImager (Scanner STORM 860; GE Healthcare), followed by densitometric quantification using ImageQuant 5.0 (Molecular Dynamics, Sunnyvale, CA, USA).

Histochemistry and Immunohistochemistry

Dewaxed thin sections (5 μm) were stained with 1% Sirius red (~ 30 minutes) to reveal total collagen in pial and intracortical microvessels. Sections were observed under a Leitz Aristoplan light microscope (Leica, Montréal, QC, Canada) and pictures acquired using a digital camera (Coolpix 4500; Nikon, Tokyo, Japan). Immunohistochemistry was carried out in dewaxed sections that underwent antigen retrieval (0.05% citraconic anhydride solution, pH = 7.4, 20 minutes, $97°C$), overnight incubation at room temperature with goat anti-collagen IV (1:300) or anti-ChAT (1:250), followed by biotinylated IgG (1 hour 30 minutes), ABC kit (1 hour 15 minutes), and the reaction was visualized with a 0.05% DAB-Nickel (Ni) solution (dark brown precipitate). Double immunodetection of cholinergic terminals and vessel contours was performed with ChAT immunodetected with DAB-Ni, followed by collagen IV in the second position using slate gray (gray blue precipitate). Sections were observed under light microscopy. Free-floating thick sections (pretreated with 1% H_2O_2, 30 minutes) were incubated with rabbit anti-collagen IV (1:400) or anti-GFAP (to mark activated astrocytes; 1:1,000), and the reactions were detected by DAB-Ni and light microscopy, or donkey anti-rabbit cyanin 2-conjugated secondary antibody (1:400) and epifluorescence light microscopy, respectively. To verify the specificity of staining, primary antibodies were either omitted or primary and secondary antibodies were prepared with 5% blocking serum.

Quantification of Staining

Digital images (two to three sections per mouse, three to five mice per group) taken under the same conditions were analyzed using the MetaMorph 6.1r3 software (Universal Imaging, Downingtown, PA, USA). The Sirius red staining intensity of pial and intracortical vessels (4 to 13 vessels per mouse) was quantified in paraffin sections and expressed as an optical density ratio against background intensity. In thick sections, the occurrence of collagen IV-positive vessels featuring structural alterations (ragged, irregular, damaged walls) was scored (0 to 3, with higher scores reflecting increasing pathology) by two independent observers, one completely blind to the identity of the sections and averaged. In low-power images, the somatosensory/cingulate cortex was manually outlined and the area occupied by GFAP-positive astrocytes quantified and expressed as the percentage GFAP-positive area. The number of ChAT-positive fibers (cell bodies were manually excluded) was quantified in high-power images of layers II to IV of the somatosensory cortex. Choline acetyltransferase terminals (dark brown) in direct contact with collagen IV-positive vessels (gray blue) were manually counted in double-immunostained sections, and expressed as the number of terminals per 100-μm vessel perimeter, the latter quantified using the ImageJ software (NIH, Bethesda, MD, USA).

Morris Water Maze

Two cohorts of elderly TGF mice under chronic pioglitazone treatment were evaluated separately in the Morris

water maze. One group of mice (cohort 1) was tested for 5 consecutive days (3 trials per day) on their ability to locate a submerged platform (1 cm) in a circular pool (25°C ± 1°C opaque water) located in a room with prominent visual cues. Mice were guided to the platform on day 1 and allowed to remain on it (5 seconds) if they exceeded the allotted time (90 seconds), as described in the study by Nicolakakis et al (2008). The other group (cohort 2) received a 3-day habituation period requiring mice to swim to a visible platform (60 seconds). The wall cues and platform location were then switched, the platform submerged (1 cm in 17°C ± 1°C opaque water), and 5 days of hidden-platform trials ensued. Two hours after hidden-platform testing, all mice were given a probe trial (60 seconds) in which the percentage time spent and distance traveled in the target quadrant (no longer containing a platform) were recorded, along with the number of crossings above the previous platform location, and swim speed. Visual acuity and motivation were tested by successful escape onto the visible platform in a separate cue trial, immediately after the probe trial (cohort 1) or during the habituation period (cohort 2). Escape latency was acquired using the 2020 Plus tracking system and Water 2020 software (Ganz FC62D video camera; HVS Image, Buckingham, UK). Animals were allowed to dry under a heating lamp after each trial to avoid hypothermia, and all experiments were started at the same time every day. Levels of serum corticosterone, a stress-induced glucocorticoid known to impair memory, were measured in cohort 1 at the time of killing, using the Correlate-EIA Corticosterone enzyme immunoassay kit, as described in the study by Nicolakakis et al (2008).

Laser Doppler Flowmetry

Laser Doppler flowmetry measurement of CBF (Transonic Systems, Ithaca, NY, USA) was carried out 2 to 3 days after the Morris water maze in elderly TGF mice anesthetized with ketamine (80 mg/kg, intraperitoneally) and fixed in a stereotaxic frame, as described previously (Nicolakakis et al, 2008). CBF before, during, and after whisker stimulation (20 seconds at 8 to 10 Hz, electric toothbrush) was recorded, with four to five recordings acquired every 30 to 40 seconds and averaged per mouse. Cortical CBF change was expressed as percentage increase relative to baseline.

2-Deoxy-2-[^{18}F]Fluoro-D-Glucose-Positron-Emission Tomography

Mice were scanned for cerebral uptake of 2-deoxy-2-[^{18}F]fluoro-D-glucose (FDG) under isoflurane sedation (1% to 2% in medical air) in a CTI Concorde R4 microPET scanner (Siemens Preclinical Solutions, Knoxville, TN, USA), as described previously (Nicolakakis et al, 2008). After a bolus injection of 1.48 to 3.33 MBq (40 to 90 μCi, 100 μL) of FDG into the tail vein, animals underwent 45 minutes of continuous whisker stimulation (8 to 10 Hz, electric toothbrush), followed by 25-min PET acquisition (15-minute emission/10-minute transmission scan using a [^{57}Co] point source). Mice were kept warm with a heating lamp and physiologic parameters maintained stable through online monitoring of cardiac rate, respiration, and temperature (Biopac Systems, Goleta, CA, USA).

Overnight fasting glycemia before scanning was comparable among groups (Supplementary Table 1). Functional metabolic images were reconstructed using a maximum a posteriori probability algorithm, and used to generate FDG standard uptake values (SUV) corrected for body weight and injected dose of radioligand. Average magnetic resonance imaging (MRI) templates from a different cohort of wild-type and TGF mice (n = 5 per group) served as anatomic guides. Magnetic resonance images were acquired with a 7-T Bruker Pharmascan system (Bruker Biospin, Ettlingen, Germany) using a 28-mm inner-diameter quadrature volume resonator, and a three-dimensional TrueFISP (True fast imaging with steady-state precession) sequence with the following parameters: matrix size = 128 × 128 × 64, field of view = 1.8 × 1.8 × 0.9 cm³, spatial resolution = 140 × 140 × 140 μm³, excitation flip angle = 30°, repetition time = 5.2 milliseconds, echo time = 2.6 milliseconds, number of excitations (NEX) = 4, number of phase cycles = 4, and total scan time = 35 minutes. The images were reconstructed using a maximum intensity algorithm, and the population averages were generated using the approach described by Lau et al (2008). Evoked CGU was expressed as a SUV ratio of the maximally activated somatosensory cortex (contralateral to whisker stimulation) to the analogous area of the ipsilateral cortex. Standard uptake value measurements from a subcortical area not targeted by whisker stimulation, i.e., the contralateral striatum, were used as indices of baseline cerebral glucose metabolism.

Statistical Analysis

Data are expressed as means ± s.e.m. and were analyzed by two-way ANOVA (analysis of variance) with transgene expression and treatment as factors, followed by Bonferroni's post hoc multiple comparison test (Bonferroni's P-values were reported if the interaction or at least one factor was significant). Two-group comparisons were analyzed by Student's t-test (GraphPad Prism 4, San Diego, CA, USA). P < 0.05 was considered significant.

Results

Pioglitazone, But Not NAC, Normalized the Function of a Fibrotic Brain Vasculature

In line with our previous findings (Tong et al, 2005), cerebral arteries from adult (12 month old) and elderly (∼18 month old) TGF mice exhibited impaired reactivity. As illustrated in the latter, arteries displayed significantly reduced dilatory responses to ACh and CGRP (with some arteries featuring constrictions) and lower constitutive NO synthesis, as evidenced by attenuated diameter decrease during NOS inhibition with L-NNA. In addition, TGF arteries featured a contractile deficit to ET-1, which was expressed only in the elderly cohort (Figure 1 and Table 1), but not yet developed in the 12-month-old group (Supplementary Figure 1, Supplementary Table 2), as previously reported by us (Tong et al, 2005). Impaired arterial responsiveness was not caused by receptor desensitization as
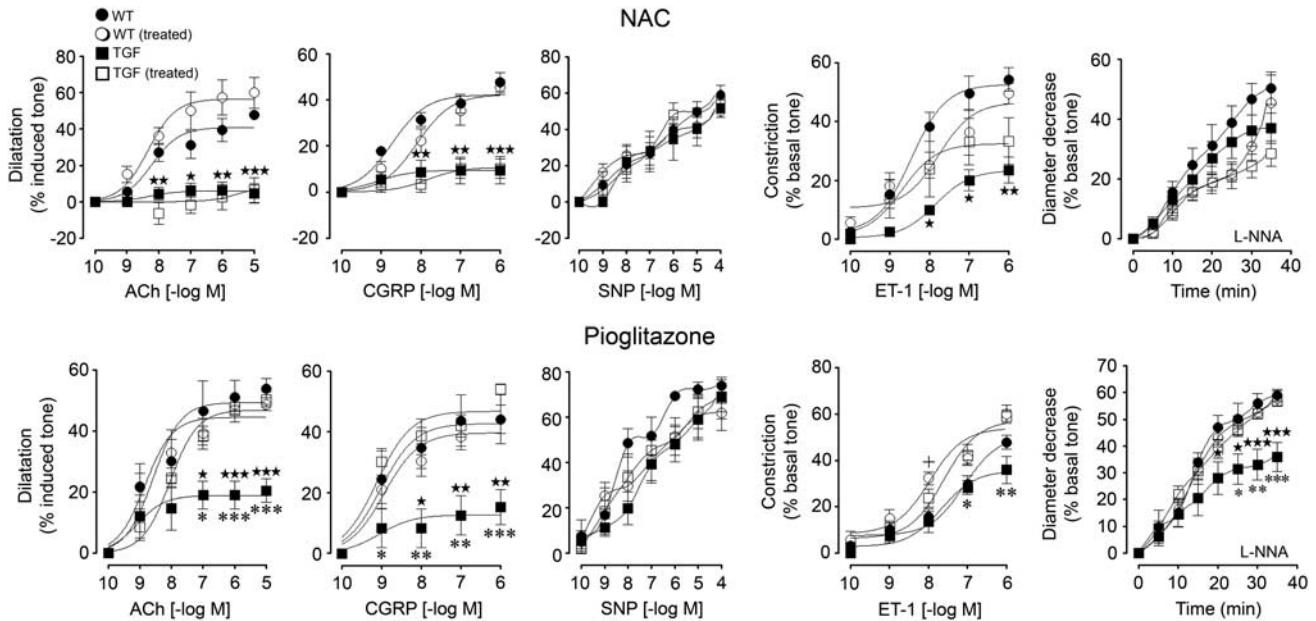
Figure 1 Effects of NAC and pioglitazone on TGF-β1-induced deficits in cerebrovascular reactivity. Early 1-year pioglitazone (pio) administration prevented the development of cerebrovascular dysfunction in adult TGF mice (data shown in Supplementary Figure 1), whereas short treatment completely reversed the established deficits of ~18-month-old TGF mice relative to their wild-type (WT) littermates (*$P < 0.05$, **$P < 0.01$, ***$P < 0.001$) in response to ACh, CGRP, ET-1, and NOS inhibition with L-NNA (10^{-5} mol/L) (untreated versus treated TGF mice, *$P < 0.05$, **$P < 0.01$, ***$P < 0.001$). Pioglitazone had no significant effect on responses of treated WT mice, except for a small enhancement of the ET-1-induced constriction (+$P < 0.05$). In contrast, NAC was ineffective on TGF-β1-induced cerebrovascular impairments. Dilatations to the nitric oxide donor SNP were comparable among groups ($n = 3$ to 7 mice per group). Errors bars represent s.e.m.

agonist potencies were largely comparable between untreated wild-type and TGF mice (Table 1 and Supplementary Table 2). Furthermore, it was also not caused by reduced protein levels of M5 mAChR or endothelial NOS (data not shown) nor by mechanical defects because arteries dilated to SNP (Figure 1). Together with the demonstration that TGF arteries normally constrict to 5-HT and phenylephrine (Tong et al, 2005; Tong and Hamel, 2007), these results highlighted the selectivity of the deficits induced by TGF-β1, and suggested downstream disturbances in vascular signaling.

In vivo treatment with NAC did not improve cerebrovascular reactivity of elderly TGF mice. This is in line with *in vitro* results from young and old isolated TGF arteries incubated with antioxidants (Tong et al, 2005), thus eliminating a role for vascular oxidative stress in the dysfunctions. In contrast, pioglitazone administered for 1 year to young pups (Supplementary Figure 1 and Supplementary Table 2) or as a short treatment to elderly TGF mice completely normalized dose-dependent and maximal agonist responses of the arteries to the dilators and the vasoconstrictor ET-1, making them comparable with or slightly enhanced relative to those of control littermates in the case of the ET-1 response (Figure 1 and Table 1). As NAC showed no benefit on vascular reactivity, we focused only on pioglitazone in subsequent investigations.

Upon dissection, the pia of adult and elderly TGF mice was thicker and more rigid than that of wild-type

littermates, as reported in previous mouse cohorts (Tong et al, 2005). This qualitative assessment was confirmed in western blots by the significant upregulation of several mediators of fibrosis, namely collagen IV, ET_B receptor, and CTGF (Figure 2A). Furthermore, microscopic examination of total collagen within vessel walls showed significant 1.7- and 1.2-fold increases in Sirius red staining intensity in the pia ($P < 0.001$) and intracortical microvessels ($P < 0.05$), respectively, of elderly TGF mice compared with wild-type controls (Figure 2B). Interestingly, short pioglitazone treatment in these mice failed to reverse parameters of remodeling (Figures 2A and 2B). Conversely, pioglitazone administered at ~4 weeks of age for 1 year prevented CTGF upregulation measured in adult TGF mice (Figure 2A), but not the rigidity of dissected vessels or structural alterations (ragged, irregular walls) evident by collagen IV immunohistochemistry (Figure 2C).

Impaired Neurovascular Coupling in Old TGF Mice and Normalization by Pioglitazone

Autoradiographic determination of baseline CBF in 9-month-old TGF mice had shown hypoperfusion in various brain areas ranging from ~20% to 33% (Gaertner et al, 2005). Correspondingly, in elderly TGF mice, the hemodynamic response to increased neuronal activity in the somatosensory cortex during whisker stimulation was significantly decreased (−24%; $P < 0.001$), but was completely restored by

Table 1 Effects of short *in vivo* NAC or pioglitazone therapy on cerebrovascular responses of elderly TGF mice to ACh, CGRP, SNP, ET-1, and NOS inhibition with L-NNA

NAC	WT (n = 4)	WT (NAC) (n = 5)	TGF (n = 7)	TGF (NAC) (n = 6)
ACh (EA_{max})	47.8 ± 2.0	60.0 ± 8.5	4.6 ± 5.4★★★	6.5 ± 6.8^a
ACh (pD_2)	8.22 ± 0.21	8.34 ± 0.22	8.31 ± 1.06	5.51 ± 2.02
CGRP (EA_{max})	47.7 ± 4.2	45.6 ± 3.2	9.5 ± 5.8★★★	10.2 ± 4.2^a
CGRP (pD_2)	8.73 ± 0.15	8.10 ± 0.19	9.08 ± 0.81	7.85 ± 0.58
SNP (EA_{max})	59.0 ± 5.5^b	50.2 ± 2.4^b	51.6 ± 4.8^b	55.8 ± 2.5^a
ET-1 (EA_{max})	54.4 ± 3.9	49.5 ± 3.5^c	$23.5 \pm 4.3^{a,}$★★	33.3 ± 7.9
ET-1 (pD_2)	8.46 ± 0.21	7.77 ± 0.33	7.84 ± 0.24	8.69 ± 0.56
L-NNA (EA_{max})	50.3 ± 5.5	45.4 ± 9.4^c	37.0 ± 5.0	28.5 ± 4.3

Pioglitazone	WT (n = 4)	WT (pio) (n = 4)	TGF (n = 4)	TGF (pio) (n = 6)
ACh (EA_{max})	54.0 ± 3.2	48.8 ± 2.0	20.4 ± 3.9★★★	50.3 ± 2.5***
ACh (pD_2)	8.58 ± 0.23	$8.84 \pm 0.20^\#$	9.09 ± 0.43	8.04 ± 0.12*
CGRP (EA_{max})	44.4 ± 8.0	44.3 ± 4.7	15.3 ± 5.8★★	54.3 ± 1.7***
CGRP (pD_2)	9.02 ± 0.30	8.93 ± 0.17	9.06 ± 0.72	9.11 ± 0.14
SNP (EA_{max})	62.0 ± 7.8	73.9 ± 2.8	68.3 ± 9.2	68.7 ± 6.3
ET-1 (EA_{max})	47.8 ± 2.9	60.0 ± 3.9	35.9 ± 5.9	58.9 ± 2.8**
ET-1 (pD_2)	7.09 ± 0.18	7.97 ± 0.20★	7.67 ± 0.27	7.60 ± 0.17
L-NNA (EA_{max})	59.0 ± 2.2	57.9 ± 2.9	35.9 ± 5.4★★★	56.7 ± 1.6***

NAC, *N*-acetyl-L-cysteine; Pio, pioglitazone; WT, wild-type.
Data are means $\pm$ s.e.m. of the number (*n*) of mice indicated in parentheses, and are expressed as maximal agonist response (EA_{max}) or potency (pD_2, $-(logEC_{50})$). EA_{max} is the percentage maximal dilatation to ACh, CGRP, and SNP, constriction to ET-1, or percentage maximal diameter decrease after 35-minute inhibition of NOS with 10^{-5} mol/L L-NNA.
★$P < 0.05$, ★★$P < 0.01$, ★★★$P < 0.001$ when compared with nontreated WT controls; *$P < 0.05$, **$P < 0.01$, ***$P < 0.001$ when compared with nontreated TGF mice; $^\#P < 0.01$ when compared with treated TGF mice.
$^a n = 5$.
$^b n = 3$.
$^c n = 4$.

short pioglitazone treatment (Figure 3A). Furthermore, both adult and elderly TGF mice featured a significant increase in GFAP-positive area in the somatosensory/cingulate cortex (Figure 3B), typical of the astrocyte activation described in this model (Wyss-Coray *et al*, 1995; Lacombe *et al*, 2004). Early, 1-year pioglitazone treatment completely reversed astroglial activation in adult animals, in line with decreased GFAP protein levels by pioglitazone in 4-month-old TGF mice (Lacombe *et al*, 2004). On the other hand, late $\sim$2-month therapy in elderly mice was ineffective (Figure 3B), suggesting that GFAP upregulation does not impede the perfusion response. In particular, it may not interfere with the ability of astrocytes to synthesize vasodilators involved in coupling CBF to increased neuronal activity (Haydon and Carmignoto, 2006).

Intact Neurometabolic Coupling During Whisker Stimulation in Elderly TGF Mice

Brain glucose consumption is a quantitative measure of neuronal activity that relies on adequate perfusion and on the glucose transporter at the blood–brain barrier. We found a tendency for decreased CGU in the striatum of elderly TGF mice (−14%; NS), and a similar trend in the striatum of pioglitazone-treated wild-type animals (−30%; NS), as measured with FDG-PET (Figure 4). These findings are in complete agreement with the decrease in basal CGU described in various limbic and sensory motor areas of TGF mice as early as 4 months of age (−12% to −22%) with the 2-deoxy [^{14}C] glucose autoradiography method (Galea *et al*, 2006), and with the diminishing effect of pioglitazone (up to −23%) reported by these authors in the most metabolically active brain areas of wild-type animals. We found no change in glucose transporter-1 protein levels by western blot (not shown), thus eliminating TGF-β1- or pioglitazone-induced glucose transporter downregulation as a factor in these changes. Interestingly, we found no impairment in the CGU response elicited by whisker stimulation in elderly TGF relative to wild-type mice (Figure 4), nor a significant reducing effect of pioglitazone. This suggested preserved neuronal activity in old transgenic animals despite hemodynamic dysfunction.
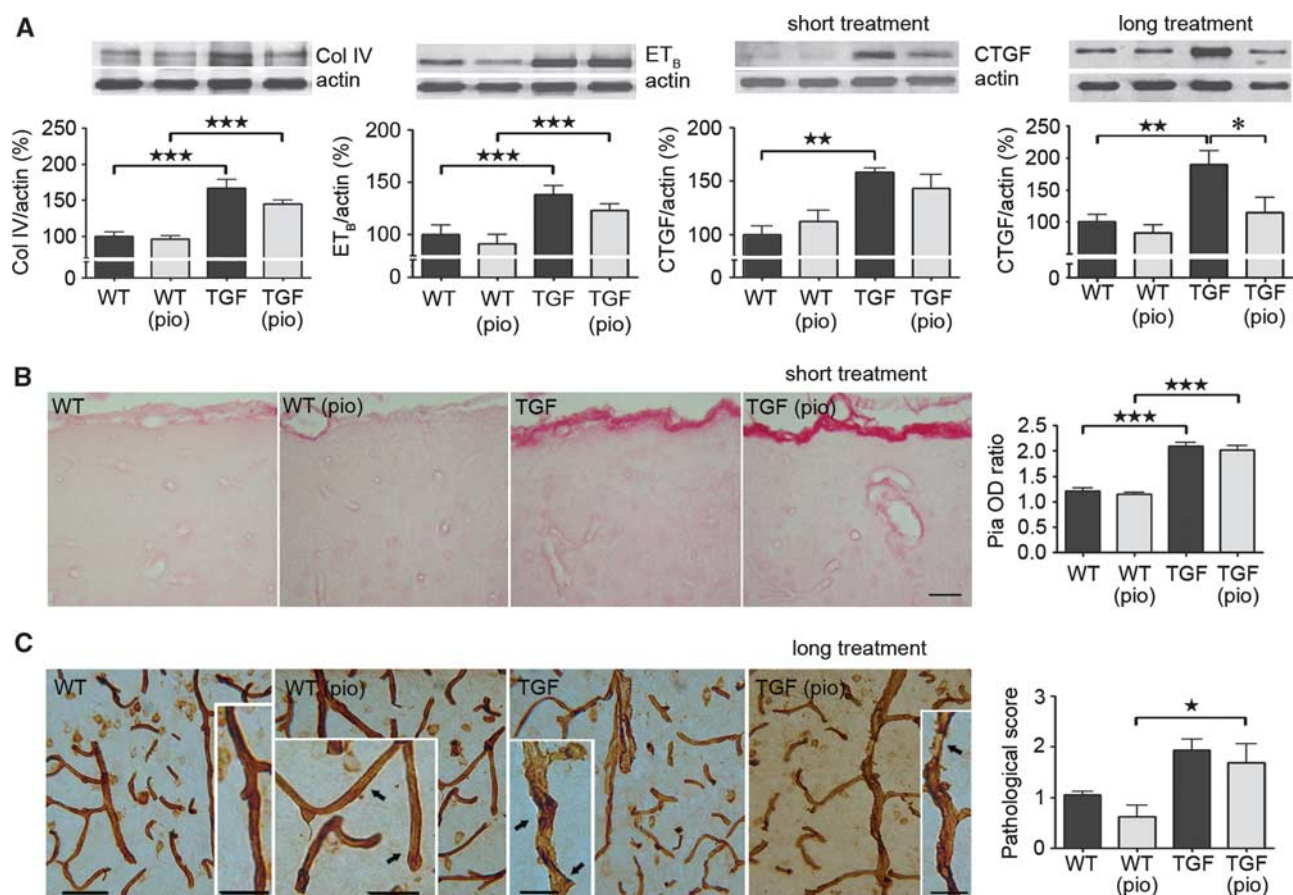
Figure 2 Pioglitazone failed to normalize vascular structure. (**A**) Short pioglitazone (pio) treatment in 18-month-old TGF mice did not reverse upregulation (★★$P < 0.01$, ★★★$P < 0.001$) of markers related to vascular fibrosis, as measured by western blot in pial vessels. However, early 1-year treatment significantly prevented (*$P < 0.05$) the increase of the TGF-β1 effector molecule CTGF. Actin was used to normalize loading variation ($n = 4$ to 6 mice per group). (**B**) Pioglitazone did not counter total collagen accumulation in the pia and intraparenchymal vessels of 18-month-old TGF mice relative to their wild-type (WT) littermates (★★★$P < 0.001$), as measured by Sirius red staining intensity in 5-μm-thick paraffin sections ($n = 3$ to 5 mice per group). Bar = 25 μm. (**C**) Similar to the unabated collagen upregulation in elderly TGF mice, structural alterations were still apparent in thick (25 μm) sections from adult transgenic animals (★$P < 0.05$) that had received early, long (1-year) pioglitazone treatment ($n = 4$ mice per group). Bars: main images = 50 μm, insets = 25 μm. Errors bars represent s.e.m.

Preserved Cholinergic and Cognitive Indices in Elderly TGF Mice

Cerebrovascular insufficiency has been associated with cholinergic and cognitive impairments (Craft *et al*, 2005), prompting us to examine these parameters in TGF mice featuring cerebrovascular dysfunction. Both the total number of ChAT-positive fibers and terminals (Figure 5A), as well as the number of perivascular ChAT terminals (Figure 5B) were comparable between elderly TGF mice and wild-type littermates, and pioglitazone had no effect, indicating the absence of a cholinergic deficit in aged TGF mice, at least with regard to this immunohistochemical assessment. Furthermore, there were no spatial memory deficits in elderly TGF mice, as measured in two separate versions of the Morris water maze. Regardless of whether animals were exposed to stress factors that could impair learning,

i.e., lack of pretraining (Figure 6A) or colder water (Figure 6B), old TGF mice and wild-type controls in both cohorts were comparable in learning and memory parameters, displaying similar escape latencies to the hidden platform and preference for the target quadrant (time and distance traveled) during the probe trial. A small decrease in the number of platform crossings was observed in TGF mice of the second cohort only (Figure 6B), reflecting a loss of precision during the search for the virtual platform. In the group that did not receive visible-platform pretraining—a habituation period that presumably reduces stress—there were no significant differences in serum corticosterone levels related to either transgene expression or treatment (wild-type, $6,718 \pm 1,774$ pg/mL; treated wild-type, $5,111 \pm 1,336$ pg/mL; TGF, $3,376 \pm 889$ pg/mL; treated TGF, $4,172 \pm 229$ pg/mL; interaction, $F_{(1,9)} = 1.052$, $P = 0.332$; transgene effect, $F(1,9) = 3.340$, $P = 0.101$;
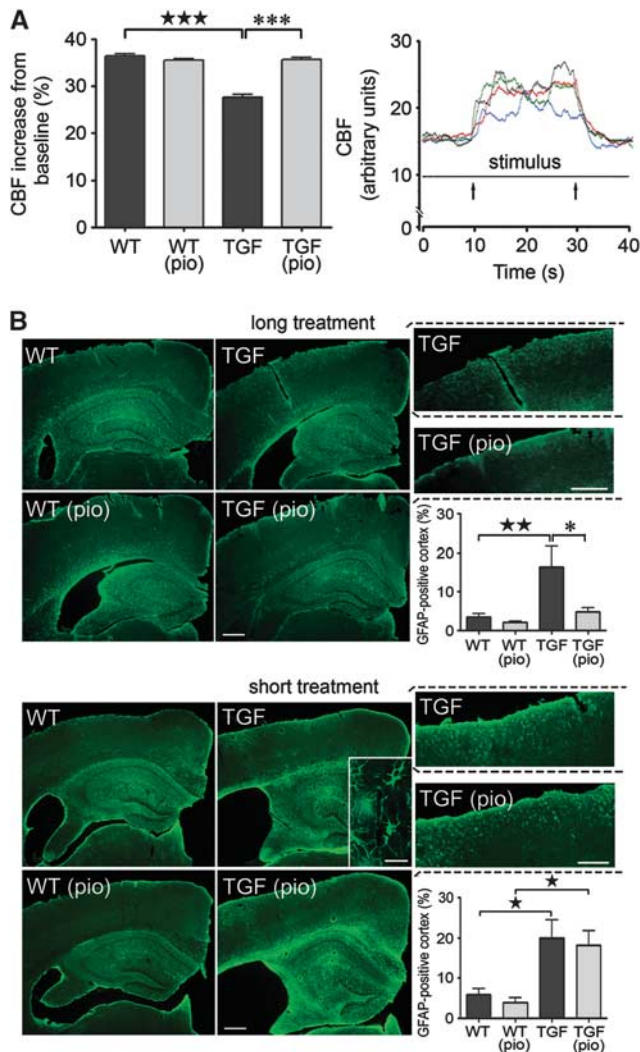
Figure 3 Pioglitazone rescued functional hyperemia and, after long treatment, normalized astrogliosis. (**A**) Short pioglitazone (pio) treatment rescued (***$P < 0.001$) the impaired neurovascular coupling response of 18-month-old TGF mice (★★★$P < 0.001$) to whisker stimulation (indicated by arrows in right panel) as measured by laser Doppler flowmetry ($n = 5$ mice per group) (traces, green: wild-type (WT); black: treated WT; blue: TGF; red: treated TGF mice). (**B**) The astrocyte activation in adult TGF mice (★★$P < 0.01$) was significantly attenuated in TGF animals treated early with pioglitazone (pio) for 1 year (*$P < 0.05$) ($n = 4$ to 5 mice per group). In contrast, short therapy in 18-month-old TGF mice did not reverse the increased percentage of cortex occupied by GFAP-positive astrocytes (★$P < 0.05$), which were readily distinguished at higher magnification (inset) ($n = 3$ to 5 mice per group). Bars: main image $= 400\,\mu m$, large inset $= 200\,\mu m$, small inset $= 25\,\mu m$. Error bars represent s.e.m.

treatment effect, $F(1,9) = 0.120$, $P = 0.737$). TGF mice also featured comparable swim speeds with wild-type counterparts, and intact visual acuity and motivation, shown by successful escape onto the visible platform. Accordingly, pioglitazone did not affect any of the mnemonic variables tested (Figure 6).

Discussion

This study brings to light the following two main findings: (1) arterial and hemodynamic dysfunction, at a comparable level with that reported in AD, did not lead to cholinergic and cognitive impairments, and (2) pioglitazone can effectively prevent or reverse cerebrovascular dysfunction in an aged, fibrotic vasculature that is resistant to antioxidant treatment. The results bear significance for the hypertensive, diabetic, stroke, and AD populations that feature TGF-β1 increase and cerebrovascular impairment, and for whom protecting the cerebral circulation could improve clinical outcome and response to therapy.

Is Cerebrovascular Dysfunction Linked to Neuronal and Cognitive Deficits?

A growing literature has been devoted to elucidate the relationship between chronic cerebral hypoperfusion and dementia, particularly in the field of AD, in which cerebrovascular dysfunction is a recognized feature of the disease (Bell and Zlokovic, 2009). Data from The Rotterdam (Ruitenberg et al, 2005) and Honolulu-Asia Aging studies (Freitag et al, 2006) have respectively shown an increased likelihood of dementia in subjects with lower middle cerebral artery blood flow velocity or with chronically restricted CBF caused by hypertension. In rodents, vessel occlusion in rats (Farkas et al, 2007; Barros et al, 2009) and vessel stenosis more recently adapted for mice (Miki et al, 2009) have led to impaired performance in tasks requiring procedural and reference memory. Nevertheless, these efforts have been unsuccessful in convincingly attributing a causative role to hypoperfusion in dementia because of the inherently correlational nature of the human studies, high degree of CBF decline created by the occlusion or stenosis paradigms, and/or the presence of confounding variables, such as cholinergic dysfunction, pyramidal cell death, or myelin loss (Farkas et al, 2007; Barros et al, 2009; Miki et al, 2009). In addition, high mortality rates (e.g., 45%), inconsistent pathologic changes that may depend on the duration of hypoperfusion or number and type of vessels occluded, as well as visual dysfunction that would preclude spatial memory testing, constitute other limitations of many occlusion models (Barros et al, 2009). In this study, we used transgenic mice featuring astrocytic TGF-β1 overexpression and consequent cerebrovascular disturbances—arterial dysfunction as early as 4 months of age (Tong et al, 2005), chronic hypoperfusion at baseline (Gaertner et al, 2005), and impaired neurovascular coupling (this study)—and showed the absence of cholinergic and cognitive deficits, as evidenced by the intact CGU response to neuronal activation, preserved immunoreactivity of the synthetic cholinergic enzyme ChAT in cortical fibers, and performance in the Morris water maze. Insofar as TGF mice constitute a model of chronic cerebrovascular deficiency, our
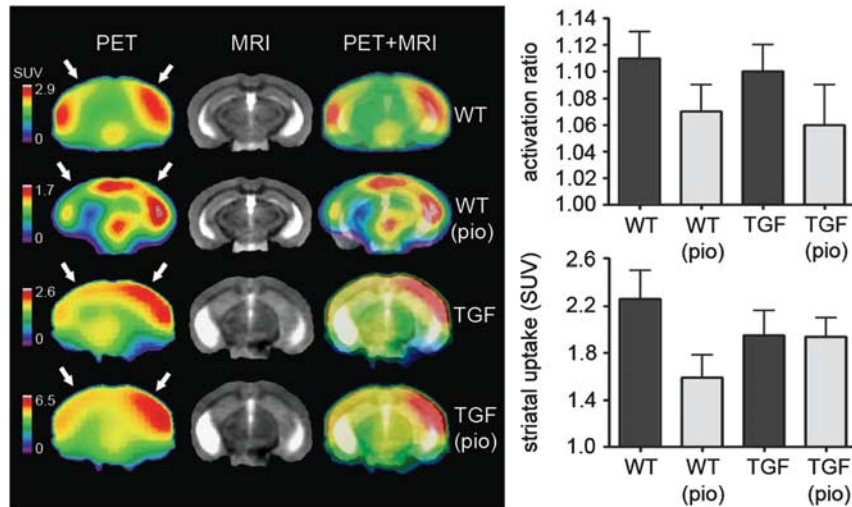
Figure 4 The cerebral glucose uptake (CGU) elicited by sensory stimulation was intact in elderly TGF mice compared with wild-type (WT) littermates, and there was no effect of pioglitazone (pio). Ratios of standard uptake value (SUV) in the activated somatosensory cortex (contralateral to whisker stimulation) relative to the analogous ipsilateral cortex were comparable among all groups. There was a tendency for reduced striatal uptake associated with TGF-$\beta1$ overexpression and pio treatment in WT mice, respectively, confirming the basal hypometabolism reported in this model (Galea et al, 2006) and induced by pio ($n = 4$ to 7 mice per group). Corresponding anatomic levels across groups were selected on the metabolic PET images using average WT and TGF MRI templates as guides. The enlarged ventricles seen in TGF brains have been reported in this model (Wyss-Coray et al, 1995). SUV scales were slightly adjusted to highlight activation ratios (arrows) in individual groups rather than the global differences across groups. Scans from representative mice are shown. Error bars represent s.e.m.
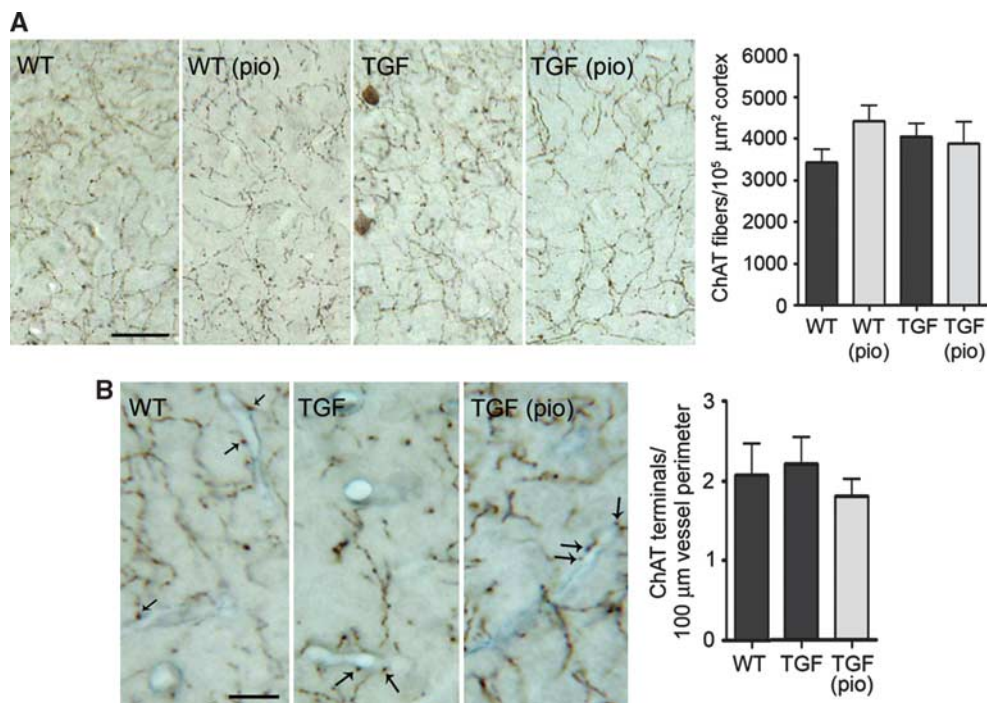
Figure 5 Total and perivascular cholinergic innervation of 18-month-old TGF mice. (**A**) The number of ChAT-positive fibers and terminals was comparable between elderly TGF and wild-type (WT) mice, and remained unaffected by short pioglitazone (pio) therapy ($n = 3$ to 5 mice per group). Bar $= 25\,\mu$m. (**B**) There was no difference in the number of cortical ChAT terminals (dark brown, indicated by arrows) apposed to collagen IV-stained vessels (blue) between WT and TGF mice, and no effect of pioglitazone ($n = 3$ to 4 mice per group). Bar $= 10\,\mu$m. Errors bars represent s.e.m.

data show that cerebrovascular dysfunction alone is insufficient to impair memory. As the level of impairment seen in TGF mice was equivalent to the

resting hypoperfusion (reviewed in Farkas and Luiten, 2001) and neurovascular coupling deficits observed in AD (10% to 30%) (Rosengarten et al,
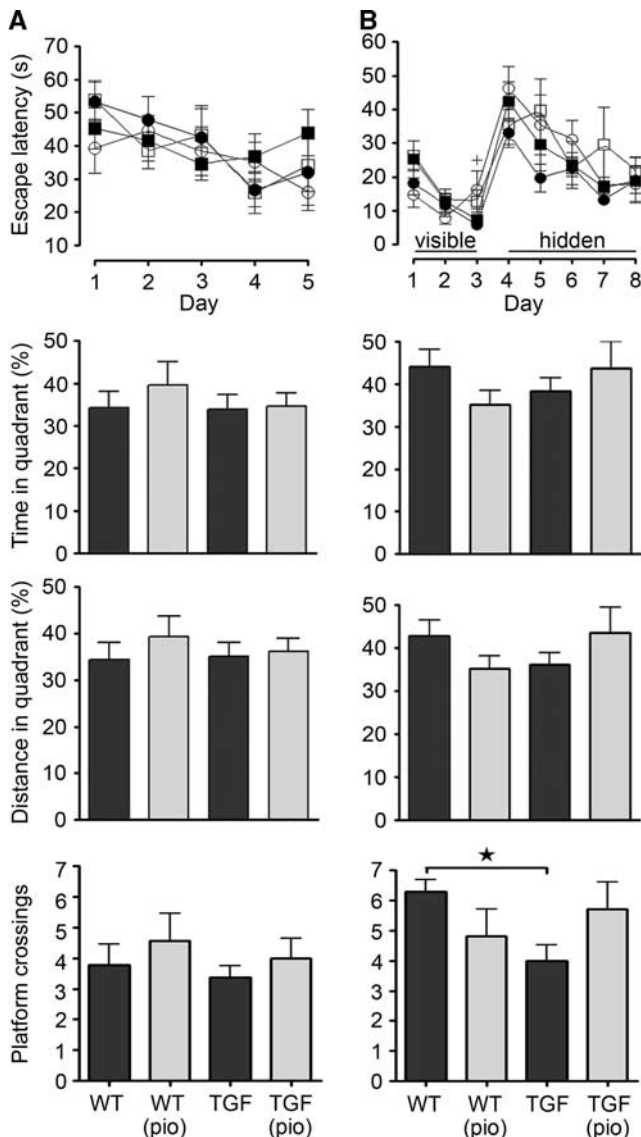
Figure 6 Despite cerebrovascular dysfunction, elderly TGF mice (■) performed as well as their wild-type (WT) counterparts (●) in two variations of the Morris water maze involving either (**A**) lack of pretraining ($n = 7$ to 11 mice per group) or (**B**) 3 days of visible-platform training ($n = 5$ to 9 mice per group). TGF-β1 expression did not affect daily escape latency, or time and traveling distance in the target quadrant during the probe trial. However, it induced a significant decrease in the number of platform crossings in cohort 2 (*$P < 0.05$). Pioglitazone (pio) had no effect on treated WT (○) or TGF (□) mice, except for a small increase in the latency of WT mice (cohort 2) on training day 3 (+$P < 0.05$). Error bars represent s.e.m.

2006), we propose that, in AD, cerebrovascular dysfunction may be an aggravating factor in the context of an underlying or concurrent cholinergic, metabolic, or amyloid pathology. This would agree with the hypoxia-induced worsening of the already-impaired memory in a mouse model of AD (Sun et al, 2006). Hence, we propose the TGF model as a simple, noninvasive alternative to the established occlusion/stenosis paradigms.

A caution to such a conclusion relates to the possible, and so far unsettled, effects of TGF-β1 on neuronal function. In this regard, some studies cite neuroprotective effects against injury, ischemia, or AD pathology in mice or AD patients (Tesseur et al, 2006; Caraci et al, 2008; Cheng et al, 2009), and others report neurodegenerative effects and impairment of spatial learning in AD mouse models (Salins et al, 2008; Town et al, 2008). As the beneficial effects of TGF-β1 may also be restricted spatially and temporally (Ueberham et al, 2005), no firm statement on its purported neuroprotective/degenerative role can be made until these data are reconciled.

Pioglitazone Protects the Aged, Fibrotic, Antioxidant-Resistant Cerebral Circulation

A most exciting finding from our study was the full recovery of cerebrovascular function in TGF mice by pioglitazone, but not by the antioxidant NAC, even though the latter had been previously shown to be efficacious in an AD mouse model featuring similar dilatory deficits to ACh and CGRP (Nicolakakis et al, 2008). The explanation relates to different mechanisms of vascular dysfunction in each mouse model. In the AD model, impaired vascular reactivity and CBF deregulation have been attributed to amyloid-β-induced oxidative stress-mediated impairment of the vasodilatory machinery and trapping of dilators by superoxide radicals (Iadecola et al, 1999; Tong et al, 2005; Nicolakakis et al, 2008). In TGF mice, western blot, immunohistochemical, cell culture, and in vitro reactivity evidence collectively preclude oxidative stress as the factor of vascular dysfunction, a finding confirmed in this study with in vivo therapy. Data point instead to altered levels or activities of vasoactive proteins and their downstream signaling cascades (Tong et al, 2005; Tong and Hamel, 2007). For example, the contractile deficit to ET-1 has been linked to upregulation of the ET-1 vasodilatory receptor ET_B, and TGF-β1-mediated inhibition of the contractile ET_A receptor/p38MAPK-HSP27 signaling pathway (this study; Tong and Hamel, 2007). Pioglitazone can restore levels of HSP27 (Park et al, 2007), enhance endothelial NOS activity (Huang et al, 2008), or directly dilate blood vessels through blockade of L-type Ca^{2+} channels in vascular smooth muscle cells (Zhang et al, 1994), hence restoring vascular dilatations to ACh and CGRP. Whatever the precise mechanism of vascular recovery, our results unambiguously show the ineffectiveness of antioxidant therapy on TGF-β1-associated cerebrovascular deficits, and strongly support the use of pioglitazone against cerebrovascular impairments associated with antioxidant resistance and TGF-β1 increase, such as in AD, hypertension, and diabetes (Grammas and Ovase, 2002; Peterson, 2005).

Another noteworthy finding was the full recovery of cerebrovascular dilatory and contractile ability in adult and elderly TGF mice, which occurred without normalization of the structural pathology. Indeed

increased levels of vascular fibrosis markers collagen IV, ET_B receptor, and CTGF associated with vessel thickening were not counteracted by pioglitazone in elderly animals. However, we cannot rule out effects on other matrix proteins, such as laminin and fibronectin, also known to be upregulated in TGF mice (Wyss-Coray *et al*, 1995). Given early as a long-term treatment, pioglitazone downregulated CTGF protein levels in adult TGF pial vessels, in agreement with a similar report in human vascular smooth muscle cells (Fu *et al*, 2001). Although this may have had a role in preventing the onset of cerebrovascular dysfunction in adult mice, it did not counter the increased rigidity and structural alterations seen in collagen IV-immunostained vessels. Taken together, these findings highlight the ability of pioglitazone to rescue cerebrovascular function even at an advanced age when vessel structure is severely altered. Furthermore, they indicate that functional and structural alterations, although they may arise from a common triggering factor, can evolve as parallel, independent facets of the initiating event, and are differentially amenable to treatment, a finding that has been highlighted in the antihypertensive drug literature (reviewed in Agabiti-Rosei *et al*, 2009). Together with the restored neurovascular coupling in elderly TGF mice, our findings underline the ability of pioglitazone to protect brain arterial function and hemodynamic regulation in the context of advanced age and fibrosis.

Conclusions

Our results draw attention to a transgenic mouse model of cerebrovascular dysfunction that can be used as an alternative to the occlusion/stenosis approaches, which are often associated with neuro-degeneration and white matter damage. Although potential TGF-β1 neuronal effects warrant further clarification, the TGF model offers a new approach toward the elucidation of the hypoperfusion–dementia relationship. Our findings further emphasize the cerebrovascular protection offered by pioglitazone to an aged arterial tree characterized by reduced cerebrovascular reactivity, impaired neurovascular coupling, fibrosis, and resistance to antioxidant treatment. Hence, our data favor the use of pioglitazone against chronic hypoperfusion in patients with AD, hypertension, or diabetes who feature TGF-β1 increase and a structurally modified vasculature.

Acknowledgements

Conflict of interest

References

Agabiti-Rosei E, Heagerty AM, Rizzoni D (2009) Effects of antihypertensive treatment on small artery remodelling. *J Hypertens* 27:1107–14

Barros CA, Ekuni R, Moro MA, Pereira FM, Dos Santos Pereira MA, Milani H (2009) The cognitive and histopathological effects of chronic 4-vessel occlusion in rats depend on the set of vessels occluded and the age of the animals. *Behav Brain Res* 197:378–87

Bell RD, Zlokovic BV (2009) Neurovascular mechanisms and blood-brain barrier disorder in Alzheimer's disease. *Acta Neuropathol* 118:103–13

Caraci F, Battaglia G, Busceti C, Biagioni F, Mastroiacovo F, Bosco P, Drago F, Nicoletti F, Sortino MA, Copani A (2008) TGF-β1 protects against Aβ-neurotoxicity via the phospha-tidylinositol-3-kinase pathway. *Neurobiol Dis* 30:234–42

Cheng JS, Dubal DB, Kim DH, Legleiter J, Cheng IH, Yu GQ, Tesseur I, Wyss-Coray T, Bonaldo P, Mucke L (2009) Collagen VI protects neurons against Aβ toxicity. *Nat Neurosci* 12:119–21

Christov A, Ottman J, Hamdheydari L, Grammas P (2008) Structural changes in Alzheimer's disease brain micro-vessels. *Curr Alzheimer Res* 5:392–5

Craft TK, Mahoney JH, Devries AC, Sarter M (2005) Microsphere embolism-induced cortical cholinergic deafferentation and impairments in attentional perfor-mance. *Eur J Neurosci* 21:3117–32

Dickson MR, Perry RT, Wiener H, Go RC (2005) Associa-tion studies of transforming growth factor-β1 and Alzheimer's disease. *Am J Med Genet (Neuropsychiatr Genet)* 139(Part B):38–41

Farkas E, Luiten PG (2001) Cerebral microvascular patho-logy in aging and Alzheimer's disease. *Progress Neuro-biol* 64:575–611

Farkas E, Luiten PG, Bari F (2007) Permanent, bilateral common carotid artery occlusion in the rat: a model for chronic cerebral hypoperfusion-related neurodegenera-tive diseases. *Brain Res Rev* 54:162–80

Freitag MH, Peila R, Masaki K, Petrovitch H, Ross GW, White LR, Launer LJ (2006) Midlife pulse pressure and incidence of dementia: the Honolulu-Asia aging study. *Stroke* 37:33–7

Fu M, Zhang J, Zhu X, Myles DE, Willson TM, Liu X, Chen YE (2001) Peroxisome proliferator-activated receptor γ inhibits transforming growth factor β-induced connective tissue growth factor expression in human aortic smooth muscle cells by interfering with Smad3. *J Biol Chem* 276:45888–94

Gaertner RF, Wyss-Coray T, Von Euw D, Lesné S, Vivien D, Lacombe P (2005) Reduced brain tissue perfusion in TGF-beta 1 transgenic mice showing Alzheimer's disease-like cerebrovascular abnormalities. *Neurobiol Dis* 19:38–46

Galea E, Feinstein DL, Lacombe P (2006) Pioglitazone does not increase cerebral glucose utilisation in a murine

model of Alzheimer's disease and decreases it in wild-type mice. *Diabetologia* 49:2153–61

Grammas P, Ovase R (2002) Cerebrovascular transforming growth factor-beta contributes to inflammation in the Alzheimer's disease brain. *Am J Pathol* 160:1583–7

Han BH, Zhou ML, Abousaleh F, Brendza RP, Dietrich HH, Koenigsknecht-Talboo J, Cirrito JR, Milner E, Holtzman DM, Zipfel GJ (2008) Cerebrovascular dysfunction in amyloid precursor protein transgenic mice: contribution of soluble and insoluble amyloid-beta peptide, partial restoration via gamma secretase inhibition. *J Neurosci* 28:13542–50.

Haydon PG, Carmignoto G (2006) Astrocyte control of synaptic transmission and neurovascular coupling. *Physiol Rev* 86:1009–31

Hirao K, Ohnishi T, Hirata Y, Yamashita F, Mori T, Moriguchi Y, Matsuda H, Nemoto K, Imabayashi E, Yamada M, Iwamoto T, Arima K, Asada T (2005) The prediction of rapid conversion to Alzheimer's disease in mild cognitive impairment using regional cerebral blood flow SPECT. *Neuroimage* 28:1014–21

Huang PH, Sata M, Nishimatsu H, Sumi M, Hirata Y, Nagai R (2008) Pioglitazone ameliorates endothelial dysfunction and restores ischemia-induced angiogenesis in diabetic mice. *Biomed Pharmacother* 62:46–52

Iadecola C, Zhang F, Niwa K, Eckman C, Turner SK, Fischer E, Younkin S, Borchelt DR, Hsiao KK, Carlson GA (1999) SOD1 rescues cerebral endothelial dysfunction in mice overexpressing amyloid precursor protein. *Nat Neurosci* 2:157–61

Krupinski J, Kumar P, Kumar S, Kaluza J (1996) Increased expression of TGF-beta 1 in brain tissue after ischemic stroke in humans. *Stroke* 27:852–7

Lacombe P, Mathews PM, Schmidt S, Breidert T, Heneka MT, Landreth GE, Feinstein DL, Galea E (2004) Effect of anti-inflammatory agents on transforming growth factor beta over-expressing mouse brains: a model revised. *J Neuroinflammation* 1:11–27

Lau JC, Lerch JP, Sled JG, Henkelman RM, Evans AC, Bedell BJ (2008) Longitudinal neuroanatomical changes determined by deformation-based morphometry in a mouse model of Alzheimer's disease. *NeuroImage* 42:19–27

Miki K, Ishibashi S, Sun L, Xu H, Ohashi W, Kuroiwa T, Mizusawa H (2009) Intensity of chronic cerebral hypoperfusion determines white/gray matter injury and cognitive/motor dysfunction in mice. *J Neurosci Res* 87:1270–81

Nicolakakis N, Aboulkassim T, Ongali B, Lecrux C, Fernandes P, Rosa-Neto P, Tong XK, Hamel E (2008) Complete rescue of cerebrovascular function in aged Alzheimer's disease transgenic mice by antioxidants and pioglitazone, a peroxisome proliferator-activated receptor γ agonist. *J Neurosci* 28:9287–96

Park SW, Yi JH, Miranpuri G, Satriotomo I, Bowen K, Resnick DK, Vemuganti R (2007) Thiazolidinedione class of peroxisome proliferator-activated receptor γ agonists prevents neuronal damage, motor dysfunction, myelin loss, neuropathic pain, and inflammation after spinal cord injury in adult rats. *J Pharmacol Exp Ther* 320:1002–12

Peterson MC (2005) Circulating transforming growth factor β-1: a partial molecular explanation for associations between hypertension, diabetes, obesity, smoking and human disease involving fibrosis. *Med Sci Monit* 11:RA229–32

Rosengarten B, Paulsen S, Molnar S, Kaschel R, Gallhofer B, Kaps M (2006) Acetylcholine esterase inhibitor donepezil improves dynamic cerebrovascular regulation in Alzheimer patients. *J Neurol* 253:58–64

Ruitenberg A, den Heijer T, Bakker SL, van Swieten JC, Koudstaal PJ, Hofman A, Breteler MM (2005) Cerebral hypoperfusion and clinical onset of dementia: the Rotterdam study. *Ann Neurol* 57:789–94

Salins P, He Y, Olson K, Glazner G, Kashour T, Amara F (2008) TGF-β1 is increased in a transgenic mouse model of familial Alzheimer's disease and causes neuronal apoptosis. *Neurosci Lett* 430:81–6

Sun X, He G, Qing H, Zhou W, Dobie F, Cai F, Staufenbiel M, Huang LE, Song W (2006) Hypoxia facilitates Alzheimer's disease pathogenesis by up-regulating BACE1 gene expression. *Proc Natl Acad Sci USA* 103:18727–32

Tesseur I, Zou K, Esposito L, Bard F, Berber E, Van Can J, Lin AH, Crews L, Tremblay P, Mathews P, Mucke L, Masliah E, Wyss-Coray T (2006) Deficiency in neuronal TGF-β signaling promotes neurodegeneration and Alzheimer's pathology. *J Clin Investigation* 116:3060–9

Tong XK, Hamel E (1999) Regional cholinergic denervation of cortical microvessels and nitric oxide synthase-containing neurons in Alzheimer's disease. *Neuroscience* 92:163–75

Tong XK, Hamel E (2007) Transforming growth factor-beta 1 impairs endothelin-1-mediated contraction of brain vessels by inducing mitogen-activated protein (MAP) kinase phosphatase-1 and inhibiting p38 MAP kinase. *Mol Pharmacol* 72:1476–83

Tong XK, Nicolakakis N, Kocharyan A, Hamel E (2005) Vascular remodeling versus amyloid β-induced oxidative stress in the cerebrovascular dysfunctions associated with Alzheimer's disease. *J Neurosci* 25:11165–74

Town T, Laouar Y, Pittenger C, Mori T, Szekely CA, Tan J, Duman RS, Flavell RA (2008) Blocking TGF-β-Smad2/3 innate immune signaling mitigates Alzheimer-like pathology. *Nat Med* 14:681–7

Ueberham U, Ueberham E, Brückner MK, Seeger G, Gärtner U, Gruschka H, Gebhardt R, Arendt T (2005) Inducible neuronal expression of transgenic TGF-β1 *in vivo*: dissection of short-term and long-term effects. *Eur J Neurosci* 22:50–64

Wyss-Coray T, Feng L, Masliah E, Ruppe MD, Lee HS, Toggas SM, Rockenstein EM, Mucke L (1995) Increased central nervous system production of extracellular matrix components and development of hydrocephalus in transgenic mice overexpressing transforming growth factor-beta 1. *Am J Pathol* 147:53–67

Wyss-Coray T, Masliah E, Mallory M, McConlogue L, Johnson-Wood K, Lin C, Mucke L (1997) Amyloidogenic role of cytokine TGF-β1 in transgenic mice and in Alzheimer's disease. *Nature* 389:603–6

Yoshida T, Ha-Kawa S, Yoshimura M, Nobuhara K, Kinoshita T, Sawada S (2007) Effectiveness of treatment with donepezil hydrochloride and changes in regional cerebral blood flow in patients with Alzheimer's disease. *Ann Nucl Med* 21:257–65

Zhang F, Sowers JR, Ram JL, Standley PR, Peuler JD (1994) Effects of pioglitazone on calcium channels in vascular smooth muscle. *Hypertension* 24:170–5